Interferometric-Processing Based Small Space Debris Imaging

Yuxue Sun[1(✉)], Ying Luo[1,2], and Song Zhang[3]

[1] Institute of Information and Navigation, Air Force Engineering University, Xi'an 710077, China
sunyuxuejiayou@163.com, luoying2002521@163.com
[2] Natural Laboratory of Radar Signal Processing, Xidian University, Xi'an 710077, China
[3] Unit 95980 of the People's Liberation Army, Xiangyang 441000, China
zhangsongl949@163.com

Abstract. The detection and recognition of small space debris is an important task for space security. This paper proposed an interferometric-processing based imaging method for small space debris. First, based on L-shaped three antennas system, the signal model for interferometric imaging is established. Then aiming at the fact that the size of some space debris is smaller than range resolution, time-frequency analysis is adopted to separate echoes of different scatterers. The mechanism of time-frequency analysis for echo from three antennas is deduced in detail. It is proved that the phase for interferometric processing is reserved in the process of time-frequency analysis. Finally through interferometric processing, the positions and image of scatterers can be reconstructed. Simulations verify the validity of the proposed method.

Keywords: Radar imaging · Interferometric processing · Space debris
Time-frequency analysis · Sinusoidal frequency modulation

1 Introduction

The space debris is a big menace of space craft, satellite, and space stations with more and more explorations in aerospace [1]. If a collision between them, the surface properties of spacecraft may be changed and great damages will be brought about. Thus it is an important task to implement space surveillance for the safety of spacecraft. For space debris smaller than 1 cm, it is possible to protect spacecraft through an appropriately designed protector. For debris whose sizes are larger than 10 cm, the U.S. Space Command has employed the space surveillance networks which are situated all over the world to monitor them [2]. Thus an important target of space surveillance is space debris whose size is 1–10 cm.

High-resolution imaging needs wide bandwidth. In order to overcome the restriction of bandwidth, Ref. [3] firstly proposes a single-range Doppler interferometry (SRDI) imaging method for spinning space debris. The improved single-range matching filtering (SRMF) method is put up based on Ref. [3] to improve the range resolution and computation complexity [4]. Reference [5] proposed a single-range

X. Gu et al. (Eds.): MLICOM 2017, Part II, LNICST 227, pp. 117–123, 2018.
https://doi.org/10.1007/978-3-319-73447-7_14

imaging (SRTI) method, which takes advantage of the phase trace to realize imaging of space debris. However, these methods can reconstruct the shape of target instead of the real position and size, since the angle between target spinning axis and radar LOS is hard to obtain.

This paper proposes an interferometric-processing based imaging method for space debris. Through time-frequency analysis, the echo of different scatterers can be separated which are inseparable in range profile for resolution restriction. Then based on three-antenna imaging system, echo of each scatter from three antennas is conducted interferometric processing on time-frequency plane. The phase information is then transformed into target position. Thus the real position and size of the target are obtained. The simulation results verify the validity of the proposed method.

2 Signal Model

L-shaped interferometric imaging system and 3-D spinning targets is given in Fig. 1. Antenna A transmits signal and antenna A, B and C receive signal. They are located in the radar coordinate system XYZ at (0, 0, 0), (L, 0, 0) and (0, 0, L), respectively. Establish the target coordinate system xyz which is originated at point O whose position is (X_c, Y_c, Z_c) in the radar coordinate system. Space debris usually rotates around its axis. A scatterer P of the target, located at (x_p, y_p, z_p), rotates with angular rotation velocity $(\omega_x, \omega_y, \omega_z)$ when undergoing a translation. Radar transmits linear modulation frequency (LFM) pulse, which is represented as

$$s\left(\hat{t}, t_m\right) = \mathrm{rect}\left(\frac{\hat{t}}{T_p}\right) \cdot \exp\left(\mathrm{j}2\pi\left(f_c t + \frac{1}{2}\mu\hat{t}^2\right)\right). \tag{1}$$

where $\mathrm{rect}\left(\frac{\hat{t}}{T_p}\right) = \begin{cases} 1, & -T_p/2 \le \hat{t} \le T_p/2 \\ 0, & \text{else} \end{cases}$, f_c is carrying frequency, T_p is pulse duration, μ is modulation rate, $\hat{t} = t - t_m$ denotes fast time and $t_m = mT$, m = 0, 1, 2, …$M - 1$ denotes slow time, in which T is pulse repetition period and M is pulse

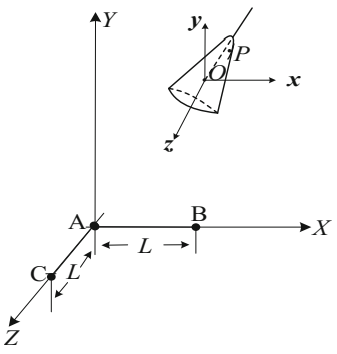

Fig. 1. Diagram of three-antenna interferometric imaging system and 3-D spinning targets.

number. After dechirp with reference range R_{AO} and Fourier transformation, the range profile of point P from antenna can be obtained as

$$\begin{aligned} S_A(f,t_m) = \sigma_p T_p \mathrm{sinc}\left(T_p\left(f+\frac{2\mu}{c}R_{\Delta AP}(t_m)\right)\right)\cdot \\ \exp\left(-\mathrm{j}\frac{4\pi}{c}f_c R_{\Delta AP}(t_m)\right). \end{aligned} \tag{2}$$

where σ_P represents scattering coefficient and $R_{\Delta AP}(t_m)$ represents the range from P to antenna A. Suppose that the translation motion has been compensated. Since the size of target is small, the echo of target should be concentrated in one range cell, that is

$$\begin{aligned} S_A(t_m) &= \sigma_p T_p \exp\left(-\mathrm{j}\frac{4\pi}{c}f_c R_{\Delta AP}(t_m)\right) \\ &= \sigma_A \exp(-\mathrm{j}\Phi_A(t_m)). \end{aligned} \tag{3}$$

where σ_A is a constant. Similarly, the echoes of antenna B and antenna C are

$$\begin{aligned} S_B(t_m) &= \sigma_p T_p \exp\left(-\mathrm{j}\frac{2\pi}{c}f_c(R_{\Delta AP}(t_m)+R_{\Delta BP}(t_m))\right) \\ &= \sigma_B \exp(-\mathrm{j}\Phi_B(t_m)). \end{aligned} \tag{4}$$

$$\begin{aligned} S_C(t_m) &= \sigma_p T_p \exp\left(-\mathrm{j}\frac{2\pi}{c}f_c(R_{\Delta AP}(t_m)+R_{\Delta CP}(t_m))\right) \\ &= \sigma_C \exp(\Phi_C(t_m)). \end{aligned} \tag{5}$$

where σ_B and σ_C are constants. Through interferometric processing, the phase difference of the range profiles between echoes from three antennas can be abstracted.

$$\begin{aligned} \mathrm{angle}(s_A(t_m)^* s_B(t_m)) &= \Phi_B(t_m) - \Phi_A(t_m) \\ &= \Delta\Phi_{AB}(t_m) \\ &= \frac{2\pi}{\lambda}(R_{\Delta AP}(t_m) - R_{\Delta BP}(t_m)). \end{aligned} \tag{6}$$

$$\begin{aligned} \mathrm{angle}(s_A(t_m)^* s_C(t_m)) &= \Phi_C(t_m) - \Phi_A(t_m) \\ &= \Delta\Phi_{AC}(t_m) \\ &= \frac{2\pi}{\lambda}(R_{\Delta AP}(t_m) - R_{\Delta CP}(t_m)). \end{aligned} \tag{7}$$

where "angle" is abstracting-phase operation and λ is wave length.

Moreover, combined with the geometrical relationship in Fig. 1, the x-axis positions and z-axis positions are obtained as

$$x(t_m) = \frac{\Delta\Phi_{AB}(t_m)\lambda \cdot R_{AO}}{2\pi L} + \frac{L}{2} - X_c. \tag{8}$$

$$z(t_m) = \frac{\Delta\Phi_{AC}(t_m)\lambda \cdot R_{AO}}{2\pi L} + \frac{L}{2} - Z_c. \tag{9}$$

3 Interferometric Processing on the Time-Frequency Plane

When there is one more scatterer in the target, all of the range profiles are stacked together in one range cell due to low range resolution. The echo of all these scatterers cannot be separated. Thus the phases of them overlay each other, in which case, interferometric processing cannot be conducted since phase term is the key for interferometric imaging. Here time-frequency analysis is adopted to separate the echoes of different scatterers, meanwhile the phase term must be reserved. Short time Fourier transform (STFT) is chosen to conduct time-frequency analysis. The definition of STFT is

$$STFT(t,f) = \int_{-\infty}^{+\infty} s(\tau)g^*(\tau - t)e^{-\mathrm{j}2\pi f\tau}d\tau. \tag{10}$$

where $g(t)$ is window function. Since the target undergoes spinning motion, $R_{\Delta AP}(t_m)$ should be a sinusoidal modulation, that is, echo of space debris as (3)–(5) is in the form of sinusoidal frequency modulation (SFM). A SFM signal can be written as

$$x(t) = \sum_{m=-\infty}^{\infty} \left\{J_m(m_f)A\ \exp[\mathrm{j}2\pi(f_c + mf_m)t]\right\}, f_m \neq 0 \quad . \tag{11}$$

where m is an integer and $J_m(\bullet)$ is the first-order Bessel function. In STFT, when a window with a relative short time width is added to SFM signal, the captured signal can be approximated as a form of LFM. For (3), the phase is

$$\Phi_A(\tau) = 2\pi f_c \frac{2R_{\Delta AP}(\tau)}{c} = 2\pi\left(f_A(t_m)\tau + \frac{1}{2}\mu_A(t_m)\tau^2\right),\ \tau \in [t_m, t_m + T_W]. \tag{12}$$

where $f_A(t_m)$ represents the initial frequency, $\mu_A(t_m)$ represents the modulation rate and T_W is time width of the window. The STFT result of (3) is

$$\begin{aligned} S_{Astft}(t_m,f) &= \int_{-\infty}^{+\infty} \sigma_A \exp(\mathrm{j}\Phi_A(\tau))g^*(\tau - t_m)e^{-\mathrm{j}2\pi f\tau}d\tau \\ &= \int_{-\infty}^{+\infty} \sigma_A \exp\left(\mathrm{j}2\pi\left(f_A(t_m)\tau + \frac{1}{2}\mu_A(t_m)\tau^2\right)\right)g^*(\tau - t_m)e^{-\mathrm{j}2\pi f\tau}d\tau. \end{aligned} \tag{13}$$

where σ_A is a constant. According to principle of stationary phase, the approximate result of (13) is

$$S_{Astft}(t_m,f) = \sigma_A g^*\left(\frac{f - f_A(t_m)}{\mu_A(t_m)} - t_m\right)\exp\left(-\mathrm{j}\frac{\pi(f - f_A(t_m))^2}{\mu_A(t_m)}\right). \tag{14}$$

Similarly, the STFT result of echo from antenna B denoted as $S_{Bstft}(t_m, f)$ and from antenna C denoted as $S_{Cstft}(t_m, f)$ can be obtained. It can be seen from (12) that the frequency of echo from antenna A is $f_A = f_A(t_m) + \mu_A(t_m)\cdot t_m$. Similarly the frequency of echo from antenna B is $f_B = f_B(t_m) + \mu_B(t_m)\cdot t_m$. Thus it yields

$$\begin{aligned}\left\{\mathrm{angle}\left(S_{Astft}(t_m,f_A)^* S_{Bstft}(t_m,f_B)\right)\right\}^* &= \pi(\mu_B(t_m) - \mu_A(t_m))t_m^2 \\ &= (\Phi_B(t_m) - \Phi_A(t_m)) - 2\pi(f_B(t_m) - f_A(t_m))t_m.\end{aligned} \tag{15}$$

The length of baseline is rather small compared with the range from target to radar, thus the time-frequency analysis result of echo from antenna A and that from antenna B are almost unanimous. Accordingly, for the same window section $[t_m, t_m + T_W]$, it yields $f_A(t_m) \approx f_B(t_m)$. In this case, (15) can be rewritten as

$$\left\{\mathrm{angle}\left(S_{Astft}(t_m,f_A)^* S_{Bstft}(t_m,f_B)\right)\right\}^* \approx \Phi_B(t_m) - \Phi_A(t_m). \tag{16}$$

Similarly, for antenna A and antenna C, it yields

$$\left\{\mathrm{angle}\left(S_{Astft}(t_m,f_A)^* S_{Cstft}(t_m,f_C)\right)\right\}^* \approx \Phi_C(t_m) - \Phi_A(t_m). \tag{17}$$

It can be seen from (16) and (17) that the interferometric phase term is still reserved after STFT analysis. And it can be abstracted directly from time-frequency plane.

4 Simulations and Analysis

Suppose that the length of baseline is L = 100 m. The carrier frequency is $f_c = 1$ GHz. Bandwidth is $B = 300$M and range resolution is 0.5 m. The imaging time is 1 s and pulse repetition frequency (PRF) is 800 Hz. The center of target is at $(0, 500, 0)$ km. There are two scatterers rotate with angular rotation velocity of $\boldsymbol{\omega} = (\pi, 2\pi, \pi)^{\mathrm{T}}\mathrm{rad/s}$. The spinning period is $T = 2\pi/\|\boldsymbol{\omega}\| = 0.2041$ s. The range profile of the target scatterers is shown in Fig. 2(a). It can be seen that range profiles of the two scatterers are concentrated in the same range cell. The STFT result is shown in Fig. 2(b).

Abstracting the phase information in STFT plane to conduct interferometric processing, the x-positions and z-positions can be reconstructed as shown in Fig. 3. It is shown in Fig. 3 that the reconstructed positions are not continuous and contain many break points. It is because that the frequency of scatterers overlaps at some seconds as shown in Fig. 2(b). At these seconds, the phase terms of different scatterers cannot be separated thus resulting failure in interferometric processing. The false reconstructed positions at these seconds are deleted. The theoretical positions are shown in Fig. 4. Compared reconstructed positions with theoretical ones, it shows that the reconstructed

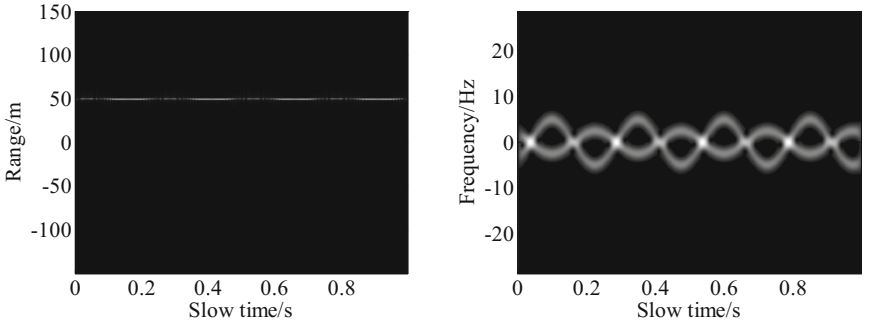

(a) the range profile (b) the result of STFT

Fig. 2. Echo processing results

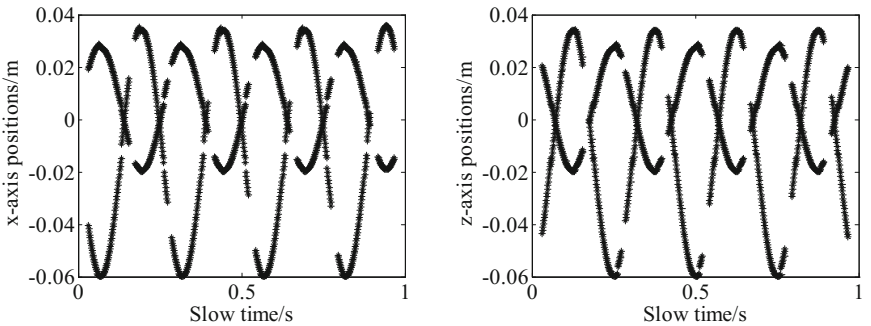

(a) reconstructed *x*-axis positions (b) reconstructed *z*-axis positions

Fig. 3. Reconstructed target positions

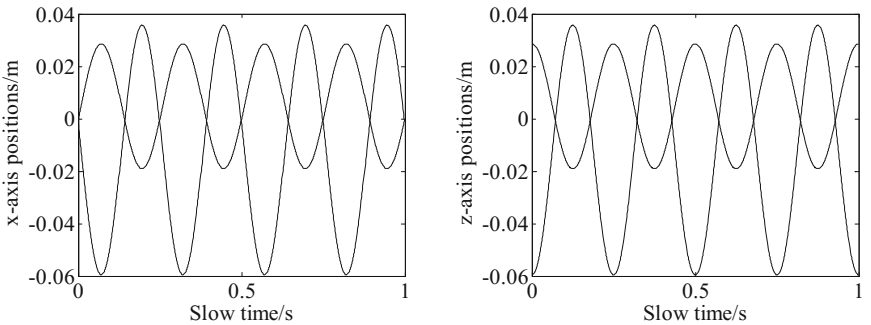

(a) theoretical *x*-axis positions (b) theoretical *z*-axis positions

Fig. 4. Theoretical target positions

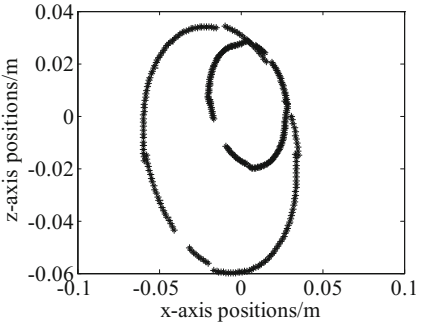

Fig. 5. Reconstructed motion trajectory

result is with good accuracy. Figure 5 is the two-dimensional motion trajectory of the target scatter. Through the motion trajectory, size and shape of the target can be scaled.

5 Conclusions

An interferometric-processing based imaging method for small space debris is offered in this paper. Through time-frequency analysis, echoes trajectories of all scatterers are segregated, which overcomes the difficulty of target size smaller than range resolution. What's more, time-frequency analysis does not destroy phase information for interferometric. Thus interferometric processing is successfully conducted to obtain the target position. The simulations verify the validity of the proposed imaging method. By comparison with existing ones, the proposed method shows the advantage that can get the real position and size of target. However, the phase information of echo is easily affected by noise. Although the space environment is in a low noise level, it is still an important task to abstract phase information in noise, which is also our next research direction.

Acknowledgments. This work was supported by the National Natural Science Foundation of China under Grant 61571457 and the Science Foundation for Post Doctorate of China under Grant 2015M570815.

References

1. Jiang, Z., Shengqi, Z., Guisheng, L.: High-resolution radar imaging of space debris base on sparse representation. J. IEEE Geosci. Remote Sens. Lett. **12**(10), 2090–2094 (2015)
2. Hongxian, W., Yinghui, Q., Mengdao, X.: Single-range image fusion for spinning space debris radar imaging. J. IEEE Geosci. Remote Sens. Lett. **7**(4), 626–630 (2010)
3. Sato, T.: Shape estimation of space debris using single-range Doppler interferometry. J. IEEE Trans. Geosci. Remote Sens. **37**(2), 1000–1005 (1999)
4. Qi, W., Mengdao, X., Guangyue, L.: Single range matching filtering for space debris radar imaging. J. IEEE Geosci. Remote Sens. Lett. **4**(4), 576–580 (2007)
5. Tao, S., Xiuming, S., Jing, C.: Three-dimensional imaging of spinning space debris based on the narrow-band radar. J. IEEE Geosci. Remote Sens. Lett. **11**(6), 1041–1045 (2014)